Peroxisome Proliferator–Activated Receptor α Protects against Glomerulonephritis Induced by Long-Term Exposure to the Plasticizer Di-(2-Ethylhexyl)Phthalate

Yuji Kamijo,[*†] Kazuhiko Hora,[†] Tamie Nakajima,[‡] Keiichi Kono,[*†] Kyoko Takahashi,[*†] Yuki Ito,[‡] Makoto Higuchi,[†] Kendo Kiyosawa,[†] Hidekazu Shigematsu,[§] Frank J. Gonzalez,[‖] and Toshifumi Aoyama[*]

*Department of Metabolic Regulation, Institute on Aging and Adaptation, †Department of Internal Medicine, and §Department of Pathology, Shinshu University School of Medicine, Matsumoto, and ‡Department of Occupational and Environmental Health, Nagoya University Graduate School of Medicine, Nagoya, Japan; and ‖Laboratory of Metabolism, National Cancer Institute, Bethesda, Maryland

Safety concerns about di-(2-ethylhexyl)phthalate (DEHP), a plasticizer and a probable endocrine disruptor, have attracted considerable public attention, but there are few studies about long-term exposure to DEHP. DEHP toxicity is thought to involve peroxisome proliferator–activated receptor α (PPARα), but this contention remains controversial. For investigation of the long-term toxicity of DEHP and determination of whether PPARα mediates toxicity, wild-type and PPARα-null mice were fed a diet that contained 0.05 or 0.01% DEHP for 22 mo. PPARα-null mice that were exposed to DEHP exhibited prominent immune complex glomerulonephritis, most likely related to elevated glomerular oxidative stress. Elevated NADPH oxidase, low antioxidant enzymes, and absence of the PPARα-dependent anti-inflammatory effects that normally antagonize the NFκB signaling pathway accompanied the glomerulonephritis in PPARα-null mice. The results reported here indicate that PPARα protects against the nephrotoxic effects of long-term exposure to DEHP.

J Am Soc Nephrol 18: 176–188, 2007. doi: 10.1681/ASN.2006060597

Di-(2-ethylhexyl)phthalate (DEHP), a probable endocrine disruptor, is used widely as a plasticizer for production of many types of polyvinyl chloride (PVC) consumer products. DEHP provides PVC items with the desired mechanical properties, including flexibility and strength. The presence of DEHP in the environment has been confirmed, as has product-related human exposure to DEHP; recent safety assessments of DEHP thereby have attracted much public interest (1). DEHP continually enters the human body via food, water, and the atmosphere. Moreover, substantial human exposure to DEHP occurs via PVC-containing medical devices that are used in intravenous therapy, enteral and parenteral nutrition support, blood transfusion, hemodialysis, cardiopulmonary bypass, and extracorporeal membrane oxygenation (2). Maximal medical exposure has been estimated to be near the US no-observed-adverse-effect level (3.7 to 14 mg/kg body wt per d). Many previous experimental animal studies yielded no obvious evidence of DEHP toxicities at these low exposure levels, but periods of exposure in the studies generally were brief. Long-term exposure to DEHP is important for safety assessment of real-world toxicity.

Past experimental animal studies using short-term exposure to high-dosage DEHP have demonstrated hepatotoxicity, testicular toxicity, renal toxicity, developmental disturbance, reproductive toxicity, and teratogenicity (3–5). The peroxisome proliferator–activated receptor α (PPARα), a member of the steroid/nuclear receptor superfamily of ligand-dependent transcription factors, has been implicated as a causative factor in these toxicities (6). PPARα is expressed abundantly in the rodent liver, testis, kidney, heart, digestive tract, and retina (7) and participates in diverse physiologic functions, including maintenance of lipid and glucose homeostasis (8–11), regulation of cell proliferation (12), and modulation of inflammatory responses (13). In humans, some ligands for this receptor, termed peroxisome proliferators, are used clinically as hypolipidemic agents, offering great benefits. However, ligand-related toxicities, such as hepatocarcinogenesis, have been observed in rodents (6). Recent studies have established that human liver contains considerably lower levels of PPARα than rodents, and this difference is thought to account for the species differences in effects of peroxisome proliferators (6). DEHP, a peroxisome proliferator, was reported to cause primarily PPARα-dependent toxicity in rodents but is considered to be relatively safe in humans. However, some studies have associated DEHP with PPARα-independent renal and testicular toxicities (14,15); accordingly, the mechanisms of DEHP toxicity as

well as the reliability of DEHP safety assessments that have been conducted to date remain controversial.

Our study was designed to accomplish two goals: To determine whether dietary exposure to DEHP (0.01 or 0.05%) for 22 mo induces toxicity and to establish the relationship between PPARα and DEHP-induced toxicity by comparing effects that were obtained between wild-type and PPARα-null mice. Long-term dietary exposure to DEHP induced glomerulonephritis in PPARα-null mice.

Materials and Methods
Animals and DEHP Treatment

PPARα-null and wild-type mice were on a SV/129 genetic background, as described elsewhere (16). These mice were maintained in a facility that was free of specific pathogens according to Shinshu University and National Institutes of Health animal care guidelines and Accreditation of Laboratory Animal Care guidelines. The mice were housed in a temperature- and light-controlled environment (25°C; 12-h light/dark cycle) and maintained on stock rodent diet and tap water *ad libitum* until reaching 12 wk of age. Twelve-week-old male wild-type and PPARα-null mice (body weight for both 25 to 30 g) were fed their regular diet or a DEHP-containing diet (0.01 or 0.05%) for 22 mo. The beginning and ending sizes of each group were as follows: $n = 25$ and 24 (one mouse died) for the control wild-type group; $n = 25$ and 23 (two mice died) for the 0.01% DEHP wild-type group; $n = 21$ and 20 (one mouse died) for the 0.05% DEHP wild-type group; $n = 26$ and 25 (one mouse died) for the control PPARα-null group; $n = 28$ and 25 (three mice died) for the 0.01% DEHP PPARα-null group; and $n = 34$ and 31 (three mice died) for the 0.05% DEHP PPARα-null group. The clinical parameters of each group of mice were checked at 0, 6, 12, and 22 mo during the experimental period. Systolic BP was measured by a programmed sphygmomanometer (BP-98A; Softron Corp., Tokyo, Japan) using a tail-cuff method. Urine protein was measured as described previously (10). Serum urea nitrogen and creatinine were determined by a clinical analyzer (JCA-BM2250; JEOL, Tokyo, Japan). All of the mice that had survived the 22-mo of experimental period were killed after finishing DEHP treatment. One PPARα-null mouse that was exposed to 0.05% DEHP exhibited marked hydronephrosis and therefore was not used in the histopathologic and biochemical analyses. The other mice showed no obvious abnormal macroscopic features, and the kidneys from these mice were used in the following analyses.

Histopathologic Analyses

Tissues from kidneys in each group of mice were fixed in 4% paraformaldehyde; embedded in paraffin; sectioned; and stained with hematoxylin and eosin, periodic acid-Schiff, or periodic acid-methenamine-silver for histopathologic examination using light microscopy. For semiquantitative histologic analyses, more than 20 glomeruli from each kidney section were examined. Degrees of cell proliferation and mesangial expansion were estimated using a scale that ranged from 0 to 3 (0, normal; 1, mild; 2, moderate; 3, severe). Indices were calculated using the following formula: Index $= (n_0 \times 0) + (n_1 \times 1) + (n_2 \times 2) + (n_3 \times 3)/\Sigma_n$ ($\Sigma_n > 20$). These histopathologic analyses were performed in a blinded manner by two observers who were unaware of the study protocol. Cryosections for immunofluorescent analyses were stained using FITC-labeled anti-mouse C3, IgG, IgA, or IgM antibodies (ICN Pharmaceuticals, Aurora, OH). Paraffin sections were deparaffinized and stained using an indirect immunoperoxidase technique. A primary mAb to a mouse macrophage marker, F4/80 antigen, was purchased from BMA Biomedicals (Augst, Switzerland). Polyclonal primary antibodies to two oxidative stress markers, 4-hydroxynonenal (4-HNE) and 8-hydroxy-2'-deoxyguanosine (8-OHdG), respectively, were purchased from Alexis Corp. (Lausen, Switzerland) and Chemicon International

(Temecula, CA). Tissues to be used for electron microscopy were fixed immediately in 2.5% glutaraldehyde, osmicated, dehydrated in increasing graded ethanol concentrations, and embedded in Epon resin. Ultrathin sections were double stained with uranyl acetate and lead citrate and examined with a JEM 1200EX II electron microscope (JEOL, Tokyo, Japan).

Immunoblot Analyses

For immunoblot analyses, glomeruli were isolated from all kidneys in each group of mice, using a previously described sieving method (17). Glomerular extracts were subjected to 9 to 15% SDS-PAGE and then transferred to nitrocellulose membranes. These membranes were incubated with primary antibody, followed by incubation with alkaline phosphatase–conjugated secondary antibody. Polyclonal primary antibodies to catalase were prepared using purified catalase (18). Primary antibodies to α-smooth muscle actin (α-SMA) and 4-HNE were purchased from DakoCytomation (Glostrup, Denmark) and Alexis Corp, respectively. Other primary antibodies, against proliferating cell nuclear antigen, TGFβ1, Nox4, p47phox, Cu,Zn-superoxide dismutase (SOD), Mn-SOD, and glutathione peroxidase, were obtained from Santa Cruz Biotechnology (Santa Cruz, CA).

Analyses of mRNA

Analyses of mRNA were performed using a real-time PCR. One microgram of total RNA was extracted from the isolated glomeruli of each group and reverse-transcribed using oligo(dT) primers and Superscript reverse transcriptase (Invitrogen, Carlsbad, CA). The cDNA were quantified with an ABI PRISM 7700 sequence detection system (Applied Biosystems, Foster City, CA), using specific primers and SYBR Green double-stranded DNA (dsDNA) binding dye I. Specific primers were designed as follows: 5'-CCTCAGGGTACCACTACGGAGT-3' and 5'-GCCGAATAGTTCGCCGAA-3' for PPARα (GenBank accession no. NM_011144); 5'-TTCCACTATGGAGTTCATGCTTGT-3' and 5'-TCCG-GCAGTTAAGATCACACCTA-3' for PPARγ (NM_011146); 5'-CACCT-GCAAGACCATCGACAT-3' and 5'-TGGCGAGCCTTAGTTTGGA-3' for TGFβ1 (NM_011577); 5'-GCCCCCGCACAGCCATGTTTCAG-3' and 5'-CATGGAGTCCAGGCCGCTGTCGTG-3' for IκBα (U36277); 5'-TGAC-CCCCAAGGCTCAAATATG-3' and 5'-ACCCAGGTCCTCGCTTATGAT-3' for cyclooxygenase2 (NM_011198); 5'-TCCGGACTTTCGATCTTCCA-3' and 5'-GAGCTTCAGAGGCAGGAAACA-3' for intercellular adhesion molecule 1 (M31585), 5'-CAGCCGATGGGTTGTACCTT-3' and 5'-GT-GGGTGAGGAGCACGTAGTC-3' for TNFα (NM_013693); 5'-CGTCCT-GACAATGCAGACCTT-3' and 5'-CCCCATGAAACGCATGAACT-3' for TNF receptor 1 (TNR1) (M60468). Glyceraldehyde-3-phosphate dehydrogenase was used as the internal control for PCR amplification.

Measurement of Serum Mono(2-Ethylhexyl)Phthalate Concentration

Serum mono(2-ethylhexyl)phthalate (MEHP) concentration was measured as described previously (19). Briefly, MEHP was extracted from serum samples with ethyl acetate. N-Methyl-N-(tert-butyl-dimethylsilyl)trifluoroacetamide (GL Sciences, Tokyo, Japan) was added to the MEHP extracts and left at room temperature for 60 min. The MEHP tert-buthyl-dimethylsilyl derivative was analyzed by gas chromatography with mass-selective detection (6890 N, 5973 N; Agilent Technologies, Santa Clara, CA). Serum samples of hemodialysis (HD) patients and healthy volunteers were collected in July 2006 with written informed consent. This study was conducted in accordance with the Declaration of Helsinki. Signed informed consent to participate in the study was obtained from all of the patients, and the study protocols

were approved by the Medical Ethics Committee of the Shinshu University School of Medicine.

Measurements of Anti-dsDNA Antibody and 50% Hemolytic Complement Activity

The titer of serum anti-dsDNA antibody was determined by ELISA as shown previously (20). The standard 50% hemolytic complement activity (CH50) was measured as described previously (21).

Statistical Analyses

Analysis of significant differences with respect to interactive effects of two factors (PPARα gene status and DEHP treatment) was performed using a two-way ANOVA. $P < 0.05$ was used as the measure of significance.

Results

DEHP Exposure Levels and Serum MEHP Concentrations

Food consumption during the experimental period was uninterrupted and similar in all groups (3.1 ± 0.7 g/d per mouse). Mean daily ingestion of DEHP approximated the maximal medical exposure in humans (8 to 11 mg/kg body wt per d for the 0.01% DEHP groups of wild-type and PPARα-null mice; 42 to 55 mg/kg body wt per d for the 0.05% DEHP groups of the two genotypes; <22.6 mg/kg body wt per d for patients undergoing therapy using PVC-containing medical devices [2]). Because most ingested DEHP is hydrolyzed efficiently by lipases to MEHP, a major DEHP metabolite whose toxicity is much more intensive than that of DEHP (2), the serum MEHP concentration in each group of mice at 22 mo was measured. The concentration increased in a DEHP dosage-dependent manner in DEHP-exposed mice of both genotypes, and there was no difference between the genotypes statistically (0.047 ± 0.014 and 0.041 ± 0.007 μg/ml for the control groups of wild-type [n = 24] and PPARα-null mice [n = 25], respectively; 0.370 ± 0.097 and 0.429 ± 0.140 μg/ml for the 0.01% DEHP groups of wild-type [n = 23] and PPARα-null mice [n = 25], respectively; 1.404 ± 0.371 and 1.737 ± 0.689 μg/ml for the 0.05% DEHP groups of wild-type [n = 20] and PPARα-null mice [n = 30], respectively). These findings suggest that the DEHP exposure levels that were chosen in this study well influence the serum concentrations of the major active metabolite, MEHP. Serum concentrations of MEHP in HD patients, who are exposed frequently to DEHP through HD sessions, were unexpectedly lower (0.056 ± 0.018 μg/ml [0.016 to 0.110 μg/ml] for the HD patients after the HD sessions [n = 109]; 0.014 ± 0.003 μg/ml for the healthy volunteers [n = 16]) than those in DEHP-exposed mice. Therefore, these findings indicate that serum MEHP concentrations probably are influenced by a species difference in DEHP metabolic efficiency.

Systemic Effects of Long-Term Dietary Exposure to DEHP

The systemic effects in all groups of mice were followed up throughout the experimental period. The levels of systolic BP, daily urinary protein excretion, serum urea nitrogen, and serum creatinine did not differ among the groups until 6 mo. Systolic BP and daily urinary protein excretion in DEHP-exposed PPARα-null mice increased in time-dependent and DEHP dosage-dependent manners after 6 mo (Figure 1, A and DEHP dosage-dependent

B). Outstanding increases of urine protein excretion in 0.01 and 0.05% DEHP-exposed PPARα-null mice were observed at both 12 and 22 mo, but the development of hypertension in 0.01% DEHP-exposed PPARα-null mice was obscure (Figure 1, A and B). Therefore, hypertension may have begun to develop after proteinuria. At 22 mo, obvious increases in serum urea nitrogen and serum creatinine in DEHP-exposed PPARα-null mice were observed in a DEHP dosage-dependent manner (Figure 1, C and D). Systolic BP and daily urinary protein excretion in exposed wild-type mice slightly increased at 22 mo, but serum urea nitrogen and serum creatinine did not change at any time during the experimental period. These data suggest DEHP-dependent renal dysfunction especially in exposed PPARα-null mice.

In all groups, body weight, kidney weight, and testicular weight were not different among the groups; however, liver weight in exposed wild-type mice at 22 mo decreased in a dosage-dependent manner (liver weight/body weight 4.28 ± 0.64% for the control wild-type group, 3.98 ± 0.45% for the 0.01% DEHP wild-type group, and 3.92 ± 0.26% for the 0.05% DEHP wild-type group). Because this effect was not observed in PPARα-null mice, the decrease in liver weight most likely reflected PPARα-dependent long-term hepatotoxicity. Because symptoms that were related to renal dysfunction were prominent, we focused on renal toxicity in the subsequent analyses.

DEHP Induces Immune-Complex Glomerulonephritis

The cause of renal dysfunction that was observed in these mice was examined by histopathologic analyses. Light microscopy using periodic acid-methenamine-silver staining demonstrated outstanding glomerular lesions with cellular proliferation and mesangial expansion in all of DEHP-exposed PPARα-null mice at 22 mo (Figure 2A). Cell proliferation and mesangial expansion in exposed PPARα-null mice increased in a dosage-dependent manner (Figure 2, B and C). Approximately 25% of PPARα-null mice that were exposed to 0.05% DEHP showed severe inflammatory findings such as mesangiolysis, mesangial edema, crescent formation, and macrophage infiltration (Figure 2, D and E). In contrast, only mild glomerular lesions were seen in DEHP-exposed wild-type mice. These findings indicate that long-term exposure to DEHP induces DEHP-dependent glomerulonephritis in PPARα-null mice.

Light microscopy also demonstrated focal tubulointerstitial lesions with tubular atrophy and inflammatory cell infiltration in DEHP-exposed PPARα-null mice. These tubulointerstitial lesions were localized around the sclerotic glomerular lesions (Figure 3). The lesions, reported in earlier studies, such as cystic tubular dilation, tubular necrosis, tubular pigmentation, and papillary mineralization (14,22), were scarcely detected here. These findings suggest that secondary tubulointerstitial lesions developed after glomerular damages occurred.

For further characterization of DEHP-induced glomerulonephritis in PPARα-null mice, immunofluorescent and electron microscopic analyses were performed. Immunofluorescence staining demonstrated C3, IgG, IgA, and IgM deposits along peripheral glomerular capillaries in DEHP-exposed PPARα-null mice at 22 mo (Figure 4A). Electron microscopic analysis
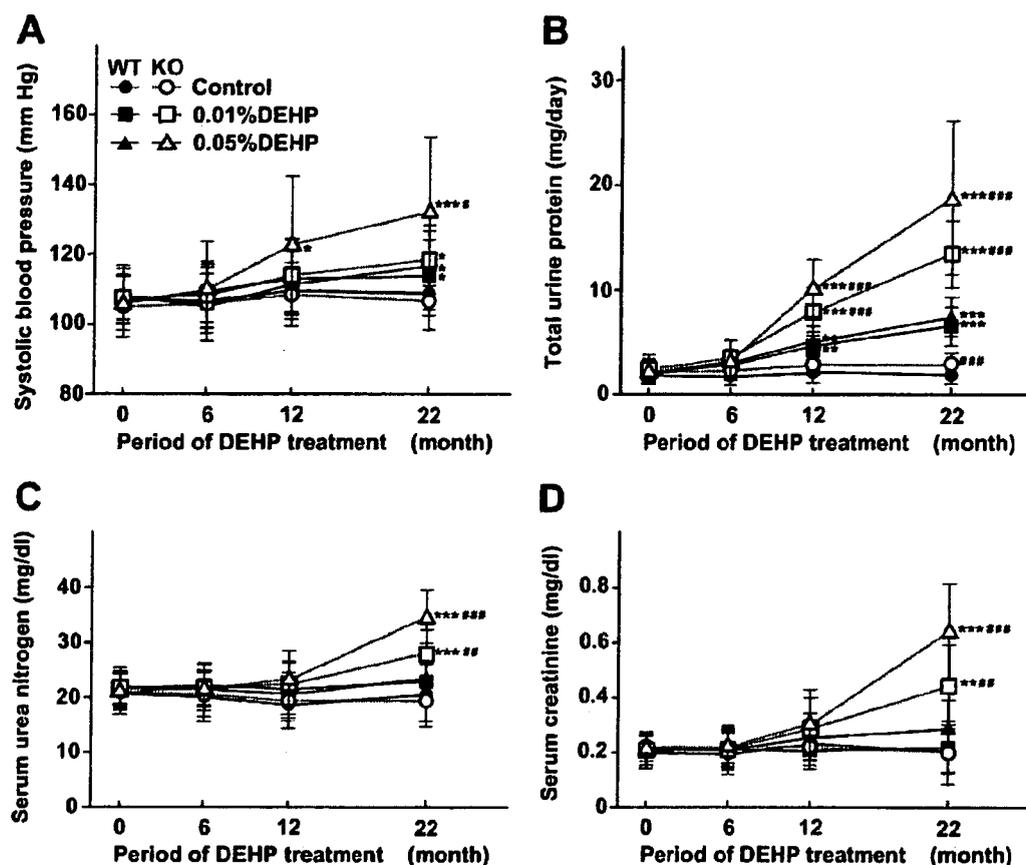
Figure 1. Effects of a diet that included di-(2-ethylhexyl)phthalate (DEHP; 0.01 or 0.05%) during 22 mo in wild-type (WT) and peroxisome proliferator–activated receptor α (PPARα)-null (KO) mice. Systolic BP (A), daily urinary protein excretion (B), serum urea nitrogen (C), and serum creatinine (D) were measured. ●, control WT group ($n = 24$); ■, 0.01% DEHP WT group ($n = 23$); ▲, 0.05% DEHP WT group ($n = 20$); ○, control KO group ($n = 25$); □, 0.01% DEHP KO group ($n = 25$); △, 0.05% DEHP KO group ($n = 30$). Data are means ± SD. *$P < 0.05$, **$P < 0.01$, ***$P < 0.001$, significantly different from the respective control group; #$P < 0.05$, ##$P < 0.01$, ###$P < 0.001$, significant differences between WT and KO mice.

revealed massive subepithelial electron-dense deposits and diffuse foot process effacement in DEHP-exposed PPARα-null mice (Figure 4B). A small number of mesangial and subendothelial deposits also were detected. In age-matched unexposed PPARα-null mice, immunofluorescence staining indicated only a few deposits in glomeruli, and electron microscopic analysis showed no abnormal changes in podocytes. These findings suggest that this glomerulonephritis involves immune mechanisms that are affected by DEHP treatment. In each mouse group, there was no appearance of anti-dsDNA antibody and no decrease in CH50. Therefore, DEHP's affecting glomerular immune-complex deposition seemed to act not systemically but renal specifically.

For further characterization of the glomerular lesions, known mediators of mesangial cell proliferation and fibrosis, specifically, α-SMA, proliferating cell nuclear antigen, and TGFβ1, were measured by immunoblotting. Expression of these proteins was increased markedly in PPARα-null mice at 22 mo in a DEHP dosage-dependent manner but increased only slightly in wild-type mice (Figure 4C). These findings are in agreement with the pathologic findings.

DEHP Elevates Oxidative Stress in Glomeruli

Because some studies have suggested that DEHP-induced elevation of oxidative stress contributes to hepatotoxicity and testicular toxicity (23–25), the influence of oxidative stress in DEHP-induced glomerulonephritis was examined. Immunoblot analysis showed that total amounts of 4-HNE–modified proteins, a lipid peroxidation marker, were increased markedly and dosage dependently in glomeruli of DEHP-exposed PPARα-null mice at 22 mo but increased only mildly in exposed wild-type mice (Figure 5A). By immunohistochemical analyses, the 4-HNE–modified proteins were detected in large numbers of podocytes in the glomeruli of DEHP-exposed PPARα-null mice at 22 mo (Figure 5B). These podocytes also contained 8-OHdG, an oxidative DNA damage marker (Figure 5C). These oxidative stress markers also showed slight positivity in parietal epithelial cells and proximal tubules of DEHP-exposed PPARα-null mice. Next, glomerular protein expression levels of two superoxide-generating NADPH oxidase subunits, Nox4 and p47phox, were examined. These proteins were increased markedly and dosage dependently in DEHP-exposed PPARα-null mice at 22 mo; these increases were present but reduced
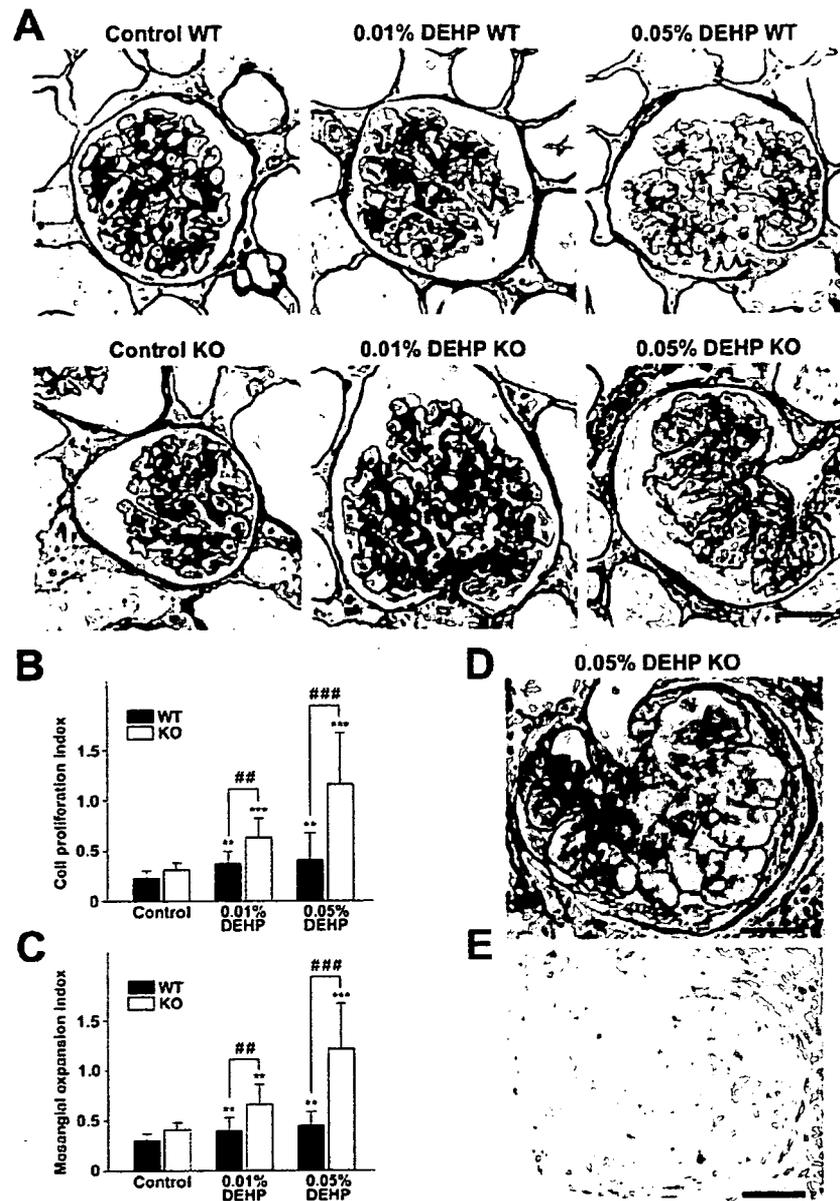
Figure 2. Light microscopic analyses of glomerular lesions. (A) Representative glomeruli from DEHP-exposed WT and KO mice at 22 mo of experiment. Sections were stained with periodic acid-methenamine-silver (PAM). Bar = 20 μm. (B and C) Indices of glomerular lesions (cell proliferation index and mesangial expansion index) at 22 mo. Data are means ± SD (n = 24 for the control WT group; n = 23 for the 0.01% DEHP WT group; n = 20 for the 0.05% DEHP WT group; n = 25 for the control KO group; n = 25 for the 0.01% DEHP KO group; n = 30 for the 0.05% DEHP KO group). **P < 0.01, ***P < 0.001, significantly different from the respective control group; ##P < 0.01, ###P < 0.001, significant differences between WT (■) and KO (□) mice. (D) Mesangiolytic and hypercellular inflammatory findings representing the glomeruli in 25% of KO mice that were exposed to 0.05% DEHP. Bar = 20 μm. (E) Immunohistochemical analysis of glomeruli in a KO mouse that was exposed to 0.05% DEHP. Deparaffinized sections were stained by an indirect immunoperoxidase technique using antibodies against mouse F4/80 (a mouse macrophage marker). Macrophages are present in intraglomerular and extracapillary spaces. Bar = 20 μm

considerably in wild-type mice (Figure 6A). The findings suggest an increase in the generation of reactive oxygen species (ROS) in glomeruli. To this end, glomerular antioxidant protein expression was measured in each group at 22 mo. Constitutive expression of catalase, Cu,Zn-SOD, and Mn-SOD was lower in unexposed PPARα-null mice than in wild-type mice; DEHP exposure further reduced glomerular expression of these proteins in PPARα-null mice (Figure 6B). Glutathione peroxidase-1 expression remained constant in all groups. These findings suggest that DEHP exposure increases oxidative stress in glomeruli, especially in podocytes, and this effect is intensified greatly in PPARα-null mice,
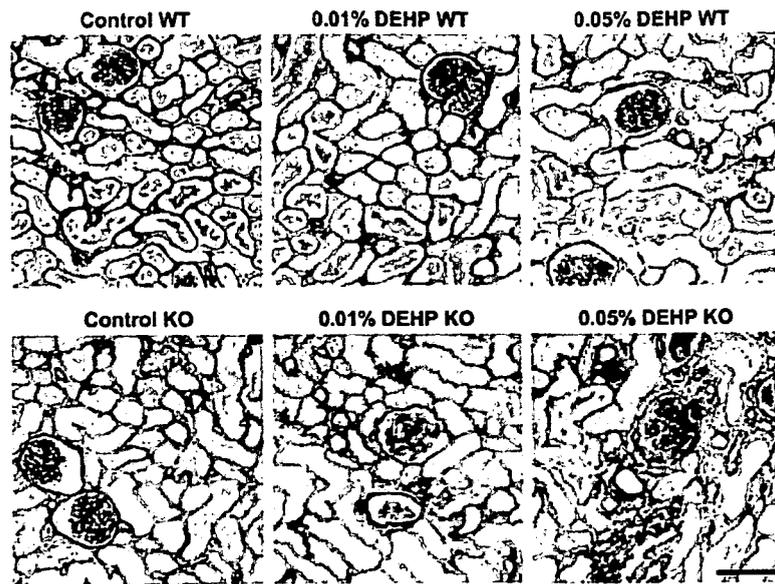
Figure 3. Light microscopic analyses of tubulointerstitial lesions. Representative tubulointerstitial findings from DEHP-exposed WT and KO mice at 22 mo of experiment. Sections were stained with PAM. Bar = 100 μm.

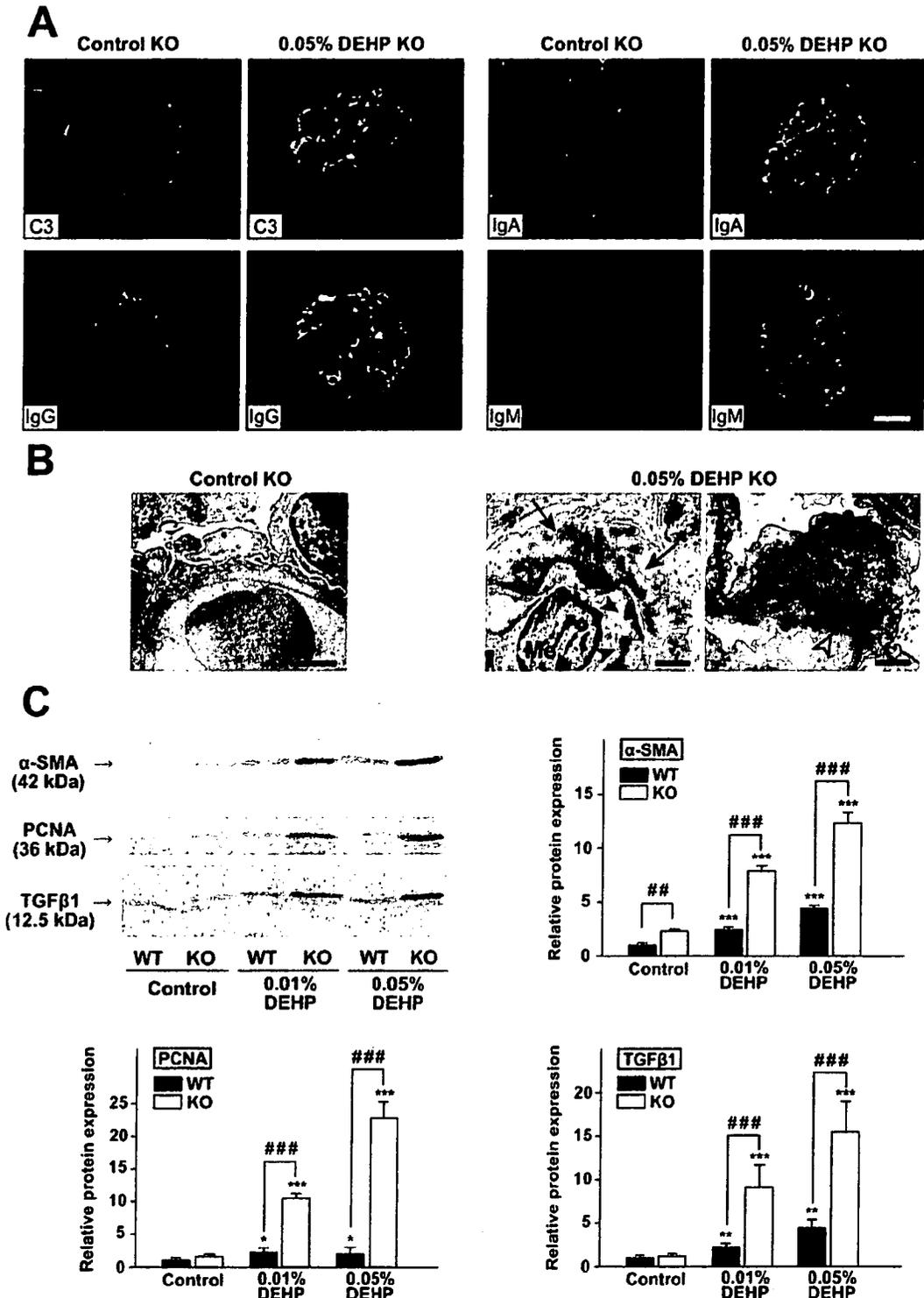reflecting their intense NADPH oxidase response and low antioxidant capabilities.

PPARα Exerts Antinephritic Effects

For investigation of the mechanism underlying development of glomerulonephritis in DEHP-exposed PPARα-null mice, expressions of mRNA encoding mediators of inflammation and fibrosis were examined, using glomerular samples at 22 mo. Because PPARα and PPARγ show anti-inflammatory effects in many tissues (13), the mRNA that encodes these transcription factors were measured using real-time PCR. As expected, glomerular expression of PPARα in PPARα-null mice remained almost undetectable throughout the experiment. Conversely, constitutive glomerular expression of PPARα in wild-type mice was high and increased in a DEHP dosage-dependent manner (Figure 7A). Constitutive glomerular expression of mRNA that encodes PPARγ, which was much less than that of PPARα in wild-type mice, did not differ between the genotypes and was decreased slightly by DEHP exposure in mice of both genotypes (Figure 7B). These findings suggest that PPARγ is not important in development of DEHP-induced glomerulonephritis. Because it was reported recently that hepatic expression of fibrogenic growth factor mRNA was influenced by PPARα expression (26), TGFβ1 mRNA was measured. Expression increased markedly in DEHP-exposed PPARα-null mice in a dosage-dependent manner, whereas the increases were only marginal in wild-type mice (Figure 7C). This mRNA expression pattern was consistent with the changes that were observed at the protein level (Figure 4C). Because PPARα is known to exert anti-inflammatory effects by inducing expression of IκBα, which antagonizes NFκB signaling (27), the expression of IκBα was measured. This mRNA was found to remain constant in exposed PPARα-null mice but increased dosage dependently in exposed wild-type mice (Figure 7D). These results were com-

patible with the observed pattern of PPARα mRNA expression. Next, the expression of mRNA that encode three proinflammatory mediators—cyclooxygenase 2, intercellular adhesion molecule 1, and TNFα, known as target molecules of the NFκB signaling pathway—were determined. Expression of the proinflammatory genes was increased considerably and dosage dependently in DEHP-exposed PPARα-null mice but was increased only mildly in exposed wild-type mice (Figure 7, E through G). In addition, the expression of TNR1 mRNA was measured to evaluate the sensitivity to the inflammatory response in PPARα-null mice. Surprising, constitutive expression of TNR1 was markedly higher in PPARα-null mice than in wild-type mice; this enhanced expression remained constant irrespective of exposure to DEHP (Figure 7H). These results suggest that PPARα exerts antinephritic effects by antagonizing the NFκB signaling pathway, preventing fibrosis, and lowering inflammatory sensitivity.

Discussion

Our study demonstrated that long-term dietary exposure to DEHP induced hypertension, proteinuria, renal dysfunction, and prominent immune-complex glomerulonephritis in PPARα-null mice. Development of glomerulonephritis seemed to be related to elevations in glomerular oxidative stress that resulted from exposure to DEHP. Glomerulonephritis was exaggerated by an increased NADPH oxidase and low antioxidant response and absence of PPARα-dependent anti-inflammatory effects, thus indicating the protection of DEHP nephrotoxicity by PPARα. DEHP-induced glomerulonephritis was found for the first time in this study. The known DEHP tubulointerstitial toxicities, reported in previous studies using high dosages of DEHP in short-term periods (14,22), did not appear in our study. The discrepancy in renal pathology between the earlier studies and this study probably is derived from differences in study design.

A

| Control KO | 0.05% DEHP KO | | Control KO | 0.05% DEHP KO |

C3 | C3 | | IgA | IgA

IgG | IgG | | IgM | IgM

B

Control KO   0.05% DEHP KO

C

α-SMA →
(42 kDa)

PCNA →
(36 kDa)

TGFβ1 →
(12.5 kDa)

WT   KO   WT   KO   WT   KO
Control   0.01%   0.05%
DEHP   DEHP

[α-SMA]
■ WT
□ KO

[PCNA]
■ WT
□ KO

[TGFβ1]
■ WT
□ KO

Figure 4. Characterization of DEHP-induced glomerulonephritis. (A) Immunofluorescence microscopic analyses of glomeruli in control and 0.05% DEHP-exposed KO mice at 22 mo of experiment. Cryosections were stained using FITC-labeled anti-mouse C3, IgG, IgA, or IgM antibodies. Bar = 20 μm. (B) Electron microscopic analysis of glomeruli in control and 0.05% DEHP-exposed KO mice at 22 mo. Arrows indicate massive subepithelial electron-dense deposits. Black arrowheads indicate mesangial deposits. White arrowhead indicates subendothelial deposits. Podocytic cytoplasm in exposed KO mice shows irregular foot process effacement. Me, mesangial cell. Bars = 2 μm. (C) Immunoblot analyses of α-smooth muscle actin (α-SMA), proliferating cell nuclear antigen (PCNA), and TGFβ1. One hundred micrograms of glomerular lysate protein that was obtained from all kidneys in each group of mice at 22 mo was used. Blots and densitometry were performed in triplicate. Data are means ± SD. $*P < 0.05$, $**P < 0.01$, $***P < 0.001$, significantly different from the respective control group; $^{\#}P <$ 0.01, $^{\#\#\#}P < 0.001$, significant differences between WT (■) and KO (□) mice.
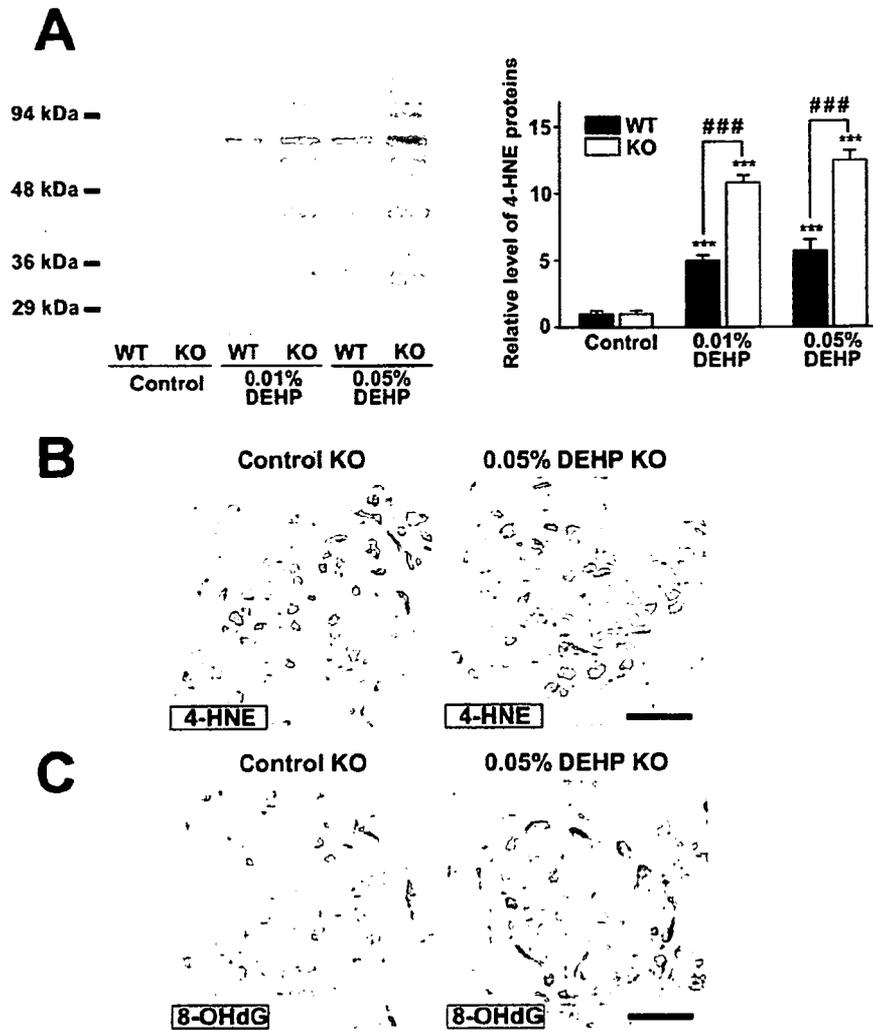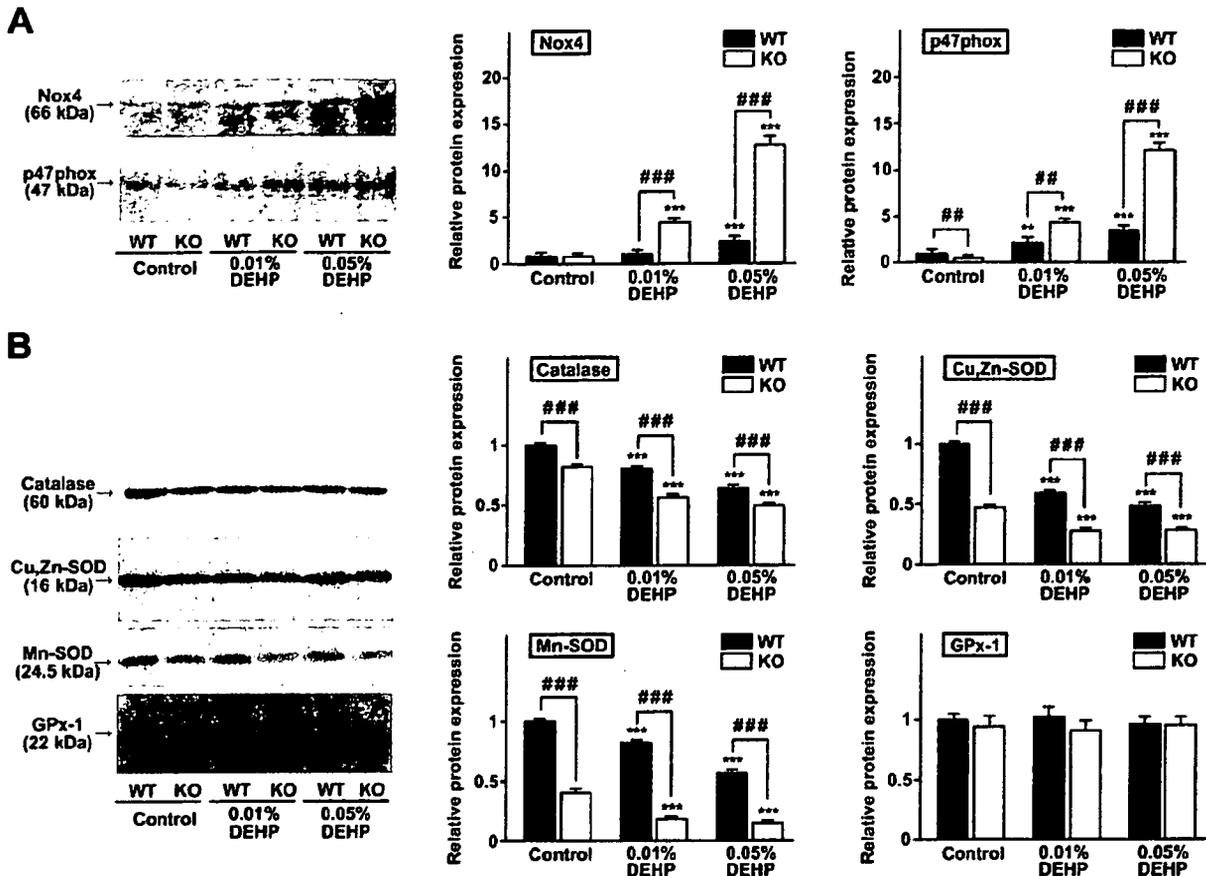
Figure 5. Changes in glomerular amounts of oxidative stress markers in DEHP-exposed WT and KO mice. (A) Immunoblot analysis of 4-HNE–modified proteins. Twenty micrograms of glomerular lysate protein that was obtained from all kidneys in each group of mice at 22 mo of experiment was used. Blotting and densitometry were performed in triplicate. Data are means ± SD. ***$P < 0.001$, significantly different from the respective control group; ###$P < 0.001$, significant difference between WT (■) and KO (□) mice. (B and C) Immunohistochemical analyses of glomeruli in control and 0.05% DEHP-exposed KO mice at 22 mo. Deparaffinized sections were stained by an indirect immunoperoxidase technique using anti–4-HNE or anti–8-OHdG antibodies. Bars = 20 μm.

It has been established that old laboratory mice exhibit the development of spontaneous subclinical immune-complex glomerulonephritis (28). In this study, a 22-mo experimental period was required for the appearance of outstanding glomerulonephritis in almost all DEHP-exposed PPARα-null mice. Therefore, the consideration of aging's effects on PPARα-null mice would be important. Indeed, a few glomerular immune-complex depositions were detected in unexposed PPARα-null mice at 22 mo. Moreover, urine protein excretion, glomerular protein expression of α-SMA, and mRNA contents of inflammatory mediators were slightly higher in these mice than in unexposed, old, wild-type mice. These findings indicate that old PPARα-null mice per se have some degree of spontaneous glomerular damages. However, these changes were very lim-

ited, as reported in an earlier study that showed spontaneous aging changes in PPARα-null mice (29). Therefore, the spontaneous aging effects probably contributed slightly to the development of glomerulonephritis in the exposed PPARα-null mice.

Oxidative stress is associated with pathophysiologic events in a variety of diseases. In particular, 4-HNE, a major end product of lipid peroxidation that exhibits a variety of cytotoxic effects in many types of cells (30), contributes to the pathogenesis of glomerulonephritis, causing injury to cell membranes of podocytes and to glomerular basement membrane (31,32). Indeed, in this study, 4-HNE and 8-OHdG were detected mainly in podocytes of DEHP-exposed PPARα-null mice, suggesting that these podocytes experienced very high levels of oxidative

Figure 6. Changes in amounts of glomerular oxidative stress–related factors in DEHP-exposed WT and KO mice. (A and B) Immunoblot analyses of Nox4, p47phox, catalase, Cu,Zn-superoxide dismutase (Cu,Zn-SOD), Mn-SOD, and glutathione peroxidase (GPx-1). Twenty micrograms of glomerular lysate protein that was obtained from all kidneys in each group of mice at 22 mo of experiment was used. Blotting and densitometry were performed in triplicate. Data are means ± SD. $^{**}P < 0.01$, $^{***}P < 0.001$, significantly different from the respective control group; $^{\#\#}P < 0.01$, $^{\#\#\#}P < 0.001$, significant differences between WT (■) and KO (□) mice.

stress. Accordingly, several pathogenic scenarios of DEHP toxicity can be postulated: (1) Lipid peroxidation that is elevated by DEHP exposure causes podocyte injury, followed by foot process effacement that entraps circulating immune complexes in the subepithelial space, leading in turn to the development of immune complex glomerulonephritis and/or (2) lipid peroxidation damages the glomerular basement membrane or cell membranes of podocytes to introduce novel antigens, followed by *in situ* immune complex formation and finally development of glomerulonephritis. Because staining for 4-HNE was slightly positive in the proximal tubules of DEHP-exposed PPARα-null mice, another pathogenic sequence, resembling events in Heymann nephritis and involving exposure of tubular antigens, may take place. Earlier studies reported that either NF-E2–related factor 2 (Nrf2) or heme-oxygenase 1–deficient mice, which were very sensitive to oxidative stress, also developed immune complex glomerulonephritis similar to our case morphologically (20,33). The development of glomerulonephritis in old Nrf2-deficient mice was practically female specific and was mediated by systemic immune disturbances, such as the appearance of anti-dsDNA antibody and the decrease of complement factors that was derived from severe oxidative stress (20). In our study using male mice, DEHP toxicities that affected glomerular immune deposits seemed to be renal specific, suggesting the presence of a nephrotoxic mechanism that is different from that in Nrf2-deficient mice. It remains unknown whether DEHP treatment causes systemic immune disturbances in PPARα-null female mice.

Our study revealed PPARα-independent effects of DEHP that resulted in enhanced activation of NADPH oxidase. To date, NADPH oxidase is the most thoroughly investigated ROS-generating system. Recent studies have implicated induction of NADPH oxidase via PPARα as the main molecular source of PPARα agonist-induced ROS (34). Contrary to these reports, our data suggest that DEHP can induce increases in glomerular NADPH oxidase proteins without involvement of PPARα. A recent study using Kupffer cells also reported that DEHP increased production of ROS in a PPARα-independent manner via NADPH oxidase (35). These results support the hypothesis that PPARα is not involved in the increase in ROS
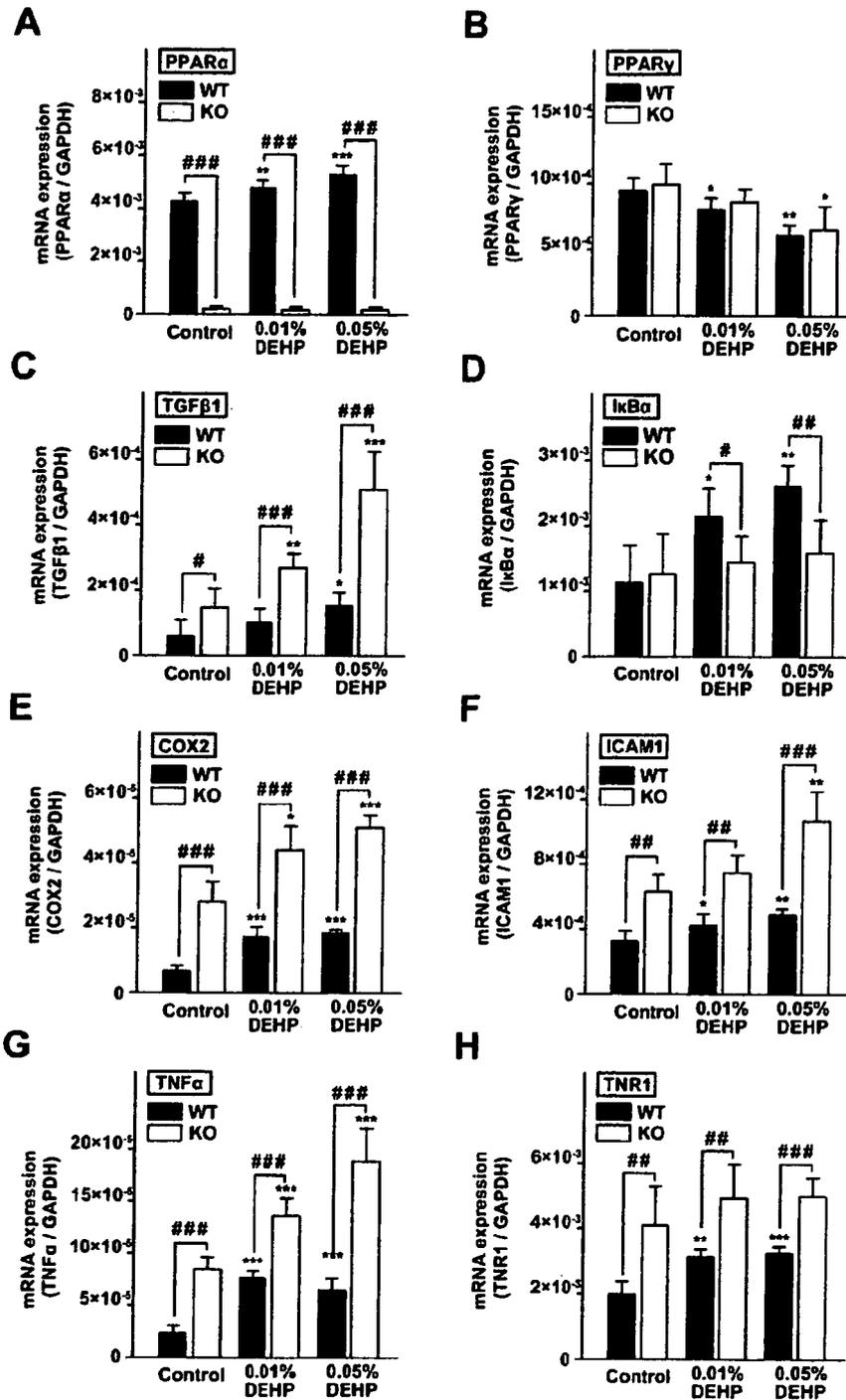
Figure 7. Changes in glomerular mRNA expression in DEHP-exposed WT and KO mice. (A through H) Analyses of mRNA in isolated glomeruli that were obtained from all kidneys in each group of mice at 22 mo of experiment. PPARα (A), PPARγ (B), TGFβ1 (C), IκBα (D), cyclooxygenase 2 (COX2; E), intercellular adhesion molecule 1 (ICAM1) (F), TNFα (G), and TNF receptor 1 (TNR1; H). The mRNA were quantified by real-time PCR. Glyceraldehyde-3-phosphate dehydrogenase mRNA was used as an internal control. Data are means ± SD of triplicate experiments. $*P < 0.05$, $**P < 0.01$, $***P < 0.001$, significantly different from the respective control group; $^\#P < 0.05$, $^{\#\#}P < 0.01$, $^{\#\#\#}P < 0.001$, significant differences between WT (■) and KO (□) mice.

that is caused by DEHP, an indicator of PPARα-independent toxicity of DEHP. Recently, a novel gp91phox homologue termed Nox4 was identified in nonphagocytic cells such as

mesangial cells (36), and this component was reported to correlate significantly with the content of α-SMA–positive cells (37). The other NADPH oxidase components, p47phox,

p22phox, and p67phox, also were reported to be induced by inflammatory stimulants in human mesangial cells (38). Because DEHP-exposed PPARα-null mice exhibited obvious mesangial cell proliferation and glomerular α-SMA protein increase, probably reflecting mesangial cell activation that was caused by excessive inflammatory mediators, these marked phenotypic changes may result in the intense glomerular NADPH oxidase response in PPARα-null mice.

Furthermore, our study revealed an interesting relationship between antioxidant activity and PPARα. It was noteworthy that constitutive expression of the antioxidant proteins such as catalase, Cu,Zn-SOD, and Mn-SOD was significantly low in PPARα-null mice and that these proteins showed decreases in response to DEHP exposure. This suggests that PPARα plays an important antioxidative role in glomeruli by contributing to the constitutive regulation of these proteins. Supporting this interpretation, the promoter regions for catalase and Cu,Zn-SOD possess PPAR response elements (39,40). No study has investigated the presence of a potential PPAR response elements in Mn-SOD gene promoter, which was characterized by a GC-rich region that contained multiple specificity protein 1 (Sp1)-binding sites (41). Several studies demonstrated that PPARα could interact with the Sp1 multigene family proteins and interfere in Sp1-dependent gene transcription (42). Therefore, PPARα may maintain transcription of Mn-SOD gene via this mechanism.

Our study also indicates that PPARα acts against DEHP-induced glomerulonephritis via transcriptional regulation of IκBα. Earlier studies established an influence of PPARα in the NFκB signaling pathway (13,27). However, the importance of PPARα in glomerulonephritis has been insufficiently recognized, because glomerular PPARα expression was reported to be low (43). A very recent report demonstrated that a large amount of PPARα existed in the nuclei of mesangial and epithelial cells in glomeruli (44), which supports the antinephritic effects of PPARα as revealed in our study. In addition to these effects, PPARα may be involved in reducing glomerular sensitivity to inflammatory mediators, because TNR1 mRNA expression was constantly higher in PPARα-null mice. Expression of TNR1 was reported to be regulated by several types of cytokines, including TNFα (45); therefore, the development of inflammation in PPARα-null mice may result from the synergistic effect of cytokines. It was suggested that all three PPAR may be novel therapeutic targets for treating renal diseases (46). Our findings may offer clues to develop renal PPAR-based disease therapies.

Taken together, our findings suggest that DEHP-induced glomerulonephritis develops if pathogenic effects of DEHP exceed the protective capacity of PPARα-dependent antinephritic effects. At present, DEHP-induced glomerulonephritis has been detected only in mice, not in humans. Moreover, our findings indicate the presence of a species difference in DEHP metabolic efficiency. Therefore, it would be difficult to evaluate our findings as a risk assessment for humans who are exposed continuously to DEHP. It remains to be determined whether the nephrotoxic effects of long-term exposure to DEHP can be reversed after withdrawal of the compound.

References

1. Center for the Evaluation of Risks to Human Reproduction: NTP-Center Expert Panel report on di-(2-ethylhexyl)-phthalate, 2000. Available at: http://cerhr.niehs.nih.gov/chemicals/dehp/DEHP-final.pdf. Accessed October 2000
2. Center for Devices and Radiological Health, US Food and Drug Administration: Safety assessment of DEHP released from PVC medical devices, 2001. Available at: http://www.fda.gov/cdrh/ost/dehp-pvc.pdf. Accessed December 2001
3. Huber WW, Grasl-Kraupp B, Schulte-Hermann R: Hepatocarcinogenic potential of di(2-ethylhexyl)phthalate in rodents and its implications on human risk. Crit Rev Toxicol 26: 365–481, 1996
4. Woodward KN: Phthalate esters, cystic kidney disease in animals and possible effects on human health: A review. Hum Exp Toxicol 9: 397–401, 1990
5. Latini G, De-Felice C, Verrotti A: Plasticizers, infant nutrition and reproductive health. Reprod Toxicol 19: 27–33, 2004
6. Gonzalez FJ, Peters JM, Cattley RC: Mechanism of action of the nongenotoxic peroxisome proliferators: Role of the peroxisome proliferator-activated receptor alpha. J Natl Cancer Inst 90: 1702–1709, 1998
7. Braissant O, Foufelle F, Scotto C, Dauca M, Wahli W: Differential expression of peroxisome proliferator-activated receptors (PPARs): Tissue distribution of PPAR-alpha, -beta, -gamma in the adult rat. Endocrinology 137: 354–366, 1996
8. Aoyama T, Peters JM, Iritani N, Nakajima T, Furihata K, Hashimoto T, Gonzalez FJ: Altered constitutive expression of fatty acid-metabolizing enzymes in mice lacking the peroxisome proliferator-activated receptor alpha (PPARalpha). J Biol Chem 273: 5678–5684, 1998
9. Watanabe K, Fujii H, Takahashi T, Kodama M, Aizawa Y, Ohta Y, Ono T, Hasegawa G, Naito M, Nakajima T, Kamijo Y, Gonzalez FJ, Aoyama T: Constitutive regulation of cardiac fatty acid metabolism through peroxisome proliferator-activated receptor alpha associated with age-dependent cardiac toxicity. J Biol Chem 275: 22293–22299, 2000
10. Kamijo Y, Hora K, Tanaka N, Usuda N, Kiyosawa K, Nakajima T, Gonzalez FJ, Aoyama T: Identification of functions of peroxisome proliferator-activated receptor alpha in proximal tubules. J Am Soc Nephrol 13: 1691–1702, 2002
11. Guerre-Millo M, Gervois P, Raspe E, Madsen L, Poulain P, Derudas B, Herbert JM, Winegar DA, Willson TM, Fruchart JC, Berge RK, Staels B: Peroxisome proliferator-activated receptor alpha activators improve insulin sensitivity and reduce adiposity. J Biol Chem 275: 16638–16642, 2000
12. Peters JM, Aoyama T, Cattley RC, Usuda N, Hashimoto T, Gonzalez FJ: Role of peroxisome proliferator-activated re-

ceptor alpha in altered cell cycle regulation in mouse liver. *Carcinogenesis* 19: 1989–1994, 1998

13. Delerive P, Fruchart JC, Staels B: Peroxisome proliferator-activated receptors in inflammation control. *J Endocrinol* 169: 453–459, 2001

14. Ward JM, Peters JM, Perella CM, Gonzalez FJ: Receptor and nonreceptor-mediated organ-specific toxicity of di(2-ethylhexyl)phthalate (DEHP) in peroxisome proliferator-activated receptor alpha-null mice. *Toxicol Pathol* 26: 240–246, 1998

15. Peters JM, Taubeneck MW, Keen CL, Gonzalez FJ: Di(2-ethylhexyl)phthalate induces a functional zinc deficiency during pregnancy and teratogenesis that is independent of peroxisome proliferator-activated receptor-alpha. *Teratology* 56: 311–316, 1997

16. Lee SS, Pineau T, Drago J, Lee EJ, Owens JW, Kroetz DL, Fernandez-Salguero PM, Westphal H, Gonzalez FJ: Targeted disruption of the alpha isoform of the peroxisome proliferator-activated receptor gene in mice results in abolishment of the pleiotropic effects of peroxisome proliferators. *Mol Cell Biol* 15: 3012–3022, 1995

17. Mori T, Bartocci A, Satriano J, Zuckerman A, Stanley R, Santiago A, Schlondorff D: Mouse mesangial cells produce colony-stimulating factor-1 (CSF-1) and express the CSF-1 receptor. *J Immunol* 144: 4697–4702, 1990

18. Furuta S, Hayashi H, Hijikata M, Miyazawa S, Osumi T, Hashimoto T: Complete nucleotide sequence of cDNA and deduced amino acid sequence of rat liver catalase. *Proc Natl Acad Sci U S A* 83: 313–317, 1986

19. Ito Y, Yamanoshita O, Kurata Y, Kamijima M, Aoyama T, Nakajima T: Induction of peroxisome proliferator-activated receptor alpha (PPARalpha)-related enzymes by di(2-ethylhexyl)phthalate (DEHP) treatment in mice and rats, but marmosets. *Arch Toxicol* August 26, 2006 [epub ahead of print]

20. Yoh K, Itoh K, Enomoto A, Hirayama A, Yamaguchi N, Kobayashi M, Morito N, Koyama A, Yamamoto M, Takahashi S: Nrf2-deficient female mice develop lupus-like autoimmune nephritis. *Kidney Int* 60: 1343–1353, 2001

21. Nangaku M, Pippin J, Couser WG: Complement membrane attack complex (C5b-9) mediates interstitial disease in experimental nephrotic syndrome. *J Am Soc Nephrol* 10: 2323–2331, 1999

22. David RM, Moore MR, Finney DC, Guest D: Chronic toxicity of di(2-ethylhexyl)phthalate in mice. *Toxicol Sci* 58: 377–385, 2000

23. Seo KW, Kim KB, Kim YJ, Choi JY, Lee KT, Choi KS: Comparison of oxidative stress and changes of xenobiotic metabolizing enzymes induced by phthalates in rats. *Food Chem Toxicol* 42: 107–114, 2004

24. Kasahara E, Sato EF, Miyoshi M, Konaka R, Hiramoto K, Sasaki J, Tokuda M, Nakano Y, Inoue M: Role of oxidative stress in germ cell apoptosis induced by di(2-ethylhexyl)phthalate. *Biochem J* 365: 849–856, 2002

25. Manojkumar V, Padmakumaran Nair KG, Santhosh A, Deepadevi KV, Arun P, Lakshmi LR, Kurup PA: Decrease in the concentration of vitamin E in blood and tissues caused by di(2-ethylhexyl)phthalate, a commonly used plasticizer in blood storage bags and medical tubing. *Vox Sang* 75: 139–144, 1998

26. Nakajima T, Kamijo Y, Tanaka N, Sugiyama E, Tanaka E, Kiyosawa K, Fukushima Y, Peters JM, Gonzalez FJ,

27. Aoyama T: Peroxisome proliferator-activated receptor α protects against alcohol-induced liver damage. *Hepatology* 40: 972–980, 2004

28. Delerive P, De Bosscher K, Vanden Berghe W, Fruchart JC, Haegeman G, Staels B: DNA binding-independent induction of IkappaBalpha gene transcription by PPARalpha. *Mol Endocrinol* 16: 1029–1039, 2002

29. Markham RV Jr, Sutherland JC, Mardiney MR Jr: The ubiquitous occurrence of immune complex localization in the glomeruli of normal mice. *Lab Invest* 29: 111–120, 1973

30. Howroyd P, Swanson C, Dunn C, Cattley RC, Corton JC: Decreased longevity and enhancement of age-dependent lesions in mice lacking the nuclear receptor peroxisome proliferator-activated receptor alpha (PPARalpha). *Toxicol Pathol* 32: 591–599, 2004

31. Esterbauer H, Schaur RJ, Zollner H: Chemistry and biochemistry of 4-hydroxynonenal, malonaldehyde and related aldehydes. *Free Radic Biol Med* 11: 81–128, 1991

32. Neale TJ, Ojha PP, Exner M, Poczewski H, Ruger B, Witztum JL, Davis P, Kerjaschki D: Proteinuria in passive Heymann nephritis is associated with lipid peroxidation and formation of adducts on type IV collagen. *J Clin Invest* 94: 1577–1584, 1994

33. Solin ML, Ahola H, Haltia A, Ursini F, Montine T, Roveri A, Kerjaschki D, Holthofer H: Lipid peroxidation in human proteinuric disease. *Kidney Int* 59: 481–487, 2001

34. Poss KD, Tonegawa S: Heme oxygenase 1 is required for mammalian iron reutilization. *Proc Natl Acad Sci U S A* 94: 10919–10924, 1997

35. Teissier E, Nohara A, Chinetti G, Paumelle R, Cariou B, Fruchart JC, Brandes RP, Shah A, Staels B: Peroxisome proliferator-activated receptor alpha induces NADPH oxidase activity in macrophages, leading to the generation of LDL with PPAR-alpha activation properties. *Circ Res* 95: 1174–1182, 2004

36. Rusyn I, Kadiiska MB, Dikalova A, Kono H, Yin M, Tsuchiya K, Mason RP, Peters JM, Gonzalez FJ, Segal BH, Holland SM, Thurman RG: Phthalates rapidly increase production of reactive oxygen species in vivo: Role of Kupffer cells. *Mol Pharmacol* 59: 744–750, 2001

37. Gorin Y, Ricono JM, Kim NH, Bhandari B, Choudhury GG, Abboud HE: Nox4 mediates angiotensin II-induced activation of Akt/protein kinase B in mesangial cells. *Am J Physiol Renal Physiol* 285: F219–F229, 2003

38. Sorescu D, Weiss D, Lassegue B, Clempus RE, Szocs K, Sorescu GP, Valppu L, Quinn MT, Lambeth JD, Vega JD, Taylor WR, Griendling KK: Superoxide production and expression of nox family proteins in human atherosclerosis. *Circulation* 105: 1429–1435, 2002

39. Jones SA, Hancock JT, Jones OT, Neubauer A, Topley N: The expression of NADPH oxidase components in human glomerular mesangial cells: Detection of protein and mRNA for p47phox, p67phox, and p22phox. *J Am Soc Nephrol* 5: 1483–1491, 1995

40. Gimun GD, Domann FE, Moore SA, Robbins ME: Identification of a functional peroxisome proliferator-activated receptor response element in the rat catalase promoter. *Mol Endocrinol* 16: 2793–2801, 2002

41. Yoo HY, Chang MS, Rho HM: Induction of the rat Cu/Zn superoxide dismutase gene through the peroxisome proliferator-responsive element by arachidonic acid. *Gene* 234: 87–91, 1999

41. Xu Y, Porntadavity S, St Clair DK: Transcriptional regulation of the human manganese superoxide dismutase gene: The role of specificity protein 1 (Sp1) and activating protein-2 (AP-2). *Biochem J* 362: 401–412, 2002

42. Gizard F, Amant C, Barbier O, Bellosta S, Robillard R, Percevault F, Sevestre H, Krimpenfort P, Corsini A, Rochette J, Glineur C, Fruchart JC, Torpier G, Staels B: PPARalpha inhibits vascular smooth muscle cell proliferation underlying intimal hyperplasia by inducing the tumor suppressor p16INK4a. *J Clin Invest* 115: 3228–3238, 2005

43. Guan Y, Zhang Y, Davis L, Breyer MD: Expression of peroxisome proliferator-activated receptors in urinary tract of rabbits and humans. *Am J Physiol* 273: F1013–F1022, 1997

44. Sato K, Sugawara A, Kudo M, Uruno A, Ito S, Takeuchi K: Expression of peroxisome proliferator-activated receptor isoform proteins in the rat kidney. *Hypertens Res* 27: 417–425, 2004

45. Alsalameh S, Mattka B, Al-Ward R, Lorenz HM, Manger B, Pfizenmaier K, Grell M, Kalden JR: Preferential expression of tumor necrosis factor receptor 55 (TNF-R55) on human articular chondrocytes: Selective transcriptional upregulation of TNF-R75 by proinflammatory cytokines interleukin 1 beta, tumor necrosis factor-alpha, and basis fibroblast growth factor. *J Rheumatol* 26: 645–653, 1999

46. Guan Y, Breyer MD: Peroxisome proliferator-activated receptors (PPARs): Novel therapeutic targets in renal disease. *Kidney Int* 60: 14–30, 2001

別添 5

研究成果の刊行に関する一覧表

雑誌

発表者氏名	論文タイトル名	発表誌名	巻	ページ	出版年
菅野純、北嶋聡、相崎健一、五十嵐勝秀、中津則之、高木篤也、小川幸男	Percellome Project による毒性トランスクリプトミクスの新しい試み	細胞工学	26	71-77	2007
菅野純、相崎健一、五十嵐勝秀、北嶋聡、中津則之、児玉幸夫、高木篤也	トキシコゲノミクスの新展開 Percellome Project による 2,3,7,8-TCDD—2,3,7,8-TCDF 比較	細胞工学	26	1391-1396	2007

PR

Percellome Projectによる毒性トランスクリプトミクスの新しい試み

菅野 純　北嶋 聡　相﨑健一　五十嵐勝秀　中津則之　高木篤也　小川幸男　児玉幸夫

別刷

Special Review

Percellome Projectによる毒性トランスクリプトミクスの新しい試み

Percellome Project as a New Approach to Toxicology Transcriptomics

菅野 純　北嶋 聡　相﨑健一　五十嵐勝秀　中津則之　高木篤也　小川幸男　児玉幸夫

Jun Kanno, Satoshi Kitajima, Ken-ichi Aisaki, Katsuhide Igarashi, Noriyuki Nakatsu, Atsuya Takagi, Yukio Ogawa, Yukio Kodama

身の回りの物質の毒性（有害性）を予測し，その被害を未然に防ぐのが毒性学の役割である．この精度向上を目指したトキシコゲノミクス研究を実施する際に，マイクロアレイなどから細胞1個当たりのmRNAコピー数を得るPercellome法を開発した．90化合物のマウス肝初期応答データを採取し終え，新たな対象（反復投与，胎児毒性，吸入毒性，多臓器連携）を加えたPercellome Projectを展開している．

key words

トキシコゲノミクス，分子毒性学，遺伝子発現カスケード，標準化，Percellome法，3次元多層（Millefeuille）データ

[i] 菅野 純　国立医薬品食品衛生研究所 安全性生物試験研究センター 毒性部　E-mail : kanno@nihs.go.jp
1985年東京医科歯科大学大学院医学研究科博士課程修了．人体病理学，実験病理学専攻．国立医薬品食品衛生研究所毒性部室長を経て，2002年より同部長．内分泌かく乱関連などの分子毒性学研究，トキシコゲノミクスプロジェクトなどを厚生労働省医薬食務との有機的連携のもとに推進．

北嶋 聡，相﨑健一，五十嵐勝秀，中津則之，高木篤也，小川幸男，児玉幸夫　国立医薬品食品衛生研究所 安全性生物試験研究センター
毒性部

はじめに

医薬品，食品，化粧品，生活関連用品など，身の回りの物質が我々の身体に取り込まれた際に生じる可能性のある毒性（有害性）を予測し，それらの使用に際しての被害を未然に防ぐのが毒性学の役割である[注1]（図1）．具体的には，人々の安全を確保するために使用法（用途）や使用量（残留量）を制限したり，場合によっては禁止したりするための科学的根拠を提供するが，その際，人の身代わりとして実験動物を用いる場合が多い．このような毒性学の精度向上の一環として，従来からの毒性研究（毒性症候学，毒性病理学，など）に加えてのトキシコゲノミクス（Toxicogenomics）研究が進められている．

トキシコゲノミクスでは，物質が生体に及ぼす影響をトランスクリプトームとして観測・解析する．その際，①分子毒性学を構築し種差や個体差の問題，複合暴露の問題などを解決するためには，遺伝子発現カスケードの全容解明を目指す必要がある，②形態学的に変化が現れた段階のトランスクリプトームは，遺伝子発現カスケードの最終段階に過ぎない，③形態変化の現れないごく初期段階を含む遺伝子発現カスケードを描出するためにはまとまった量のデータの蓄積が必須である，との観点から，筆者らは，マイクロアレイや定量PCRから細胞1個当たりのmRNAコピー数を得るPercellome手法と，そのデータ解析のための3次元多

層（Millefeuille）システムを開発・実用化した．遺伝子発現量が共通の尺度，すなわち"コピー数／細胞"で表現されることから，検体間，実験間，マイクロアレイのバージョン間，異なったプラットホーム間，などのデータ比較が直接的に行えるようになり，数年かけて蓄積したデータの有機的活用が可能となった．現在，90種類の化学物質によるマウス肝の初期応答データを採取し終えたところである．新たな対象（反復投与，胎児毒性，吸入毒性，多臓器連携）を加えたPercellome Projectの概要を紹介する．

I．Percellome法：細胞1個当たりのmRNA絶対量を得る方法

原理は単純である．サンプルの細胞数を計測し，外部標準mRNA（スパイクRNA）を細胞1個当たり決まった分子数だけそのサンプルに添加し，そしてRNA抽出，測定に移る．サンプルのRNAの測定値を，スパイクRNAの値を基準に，細胞1個当たりのコピー数に換算する．実際には細胞数を直接計測するのが困難なことが多いため，その代替指標として細胞核内のゲノムDNA量を用いる[1, 2]．定量性・直線性の検証にはLBM標準サンプル（肝[L]と脳[B]を100：0，75：25，50：50，25：75および0：100に混合した5サンプルから成るセット）を用いる．なお，スパイクRNAは，5種類の枯草菌遺伝子のmRNAを濃度公比3で混合したカクテル（dose-graded spike cocktail；GSC）として用意した．高精度を要求されるDNA定量法は手作業プロトコールおよび自動ロボット（PerkinElmer JANUS）のプロトコールを準備
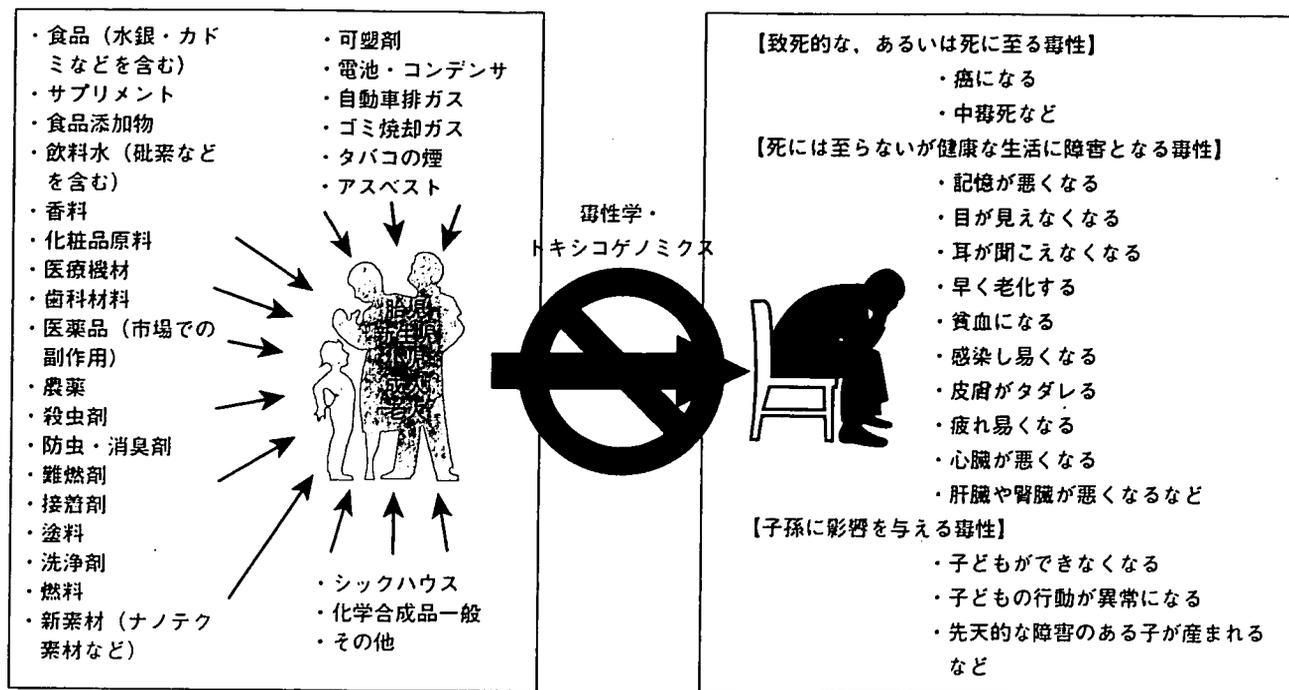

注1　環境への配慮も含まれる．

・食品（水銀・カドミなどを含む）
・サプリメント
・食品添加物
・飲料水（砒素などを含む）
・香料
・化粧品原料
・医療機材
・歯科材料
・医薬品（市場での副作用）
・農薬
・殺虫剤
・防虫・消臭剤
・難燃剤
・接着剤
・塗料
・洗浄剤
・燃料
・新素材（ナノテク素材など）

・可塑剤
・電池・コンデンサ
・自動車排ガス
・ゴミ焼却ガス
・タバコの煙
・アスベスト

・シックハウス
・化学合成品一般
・その他

毒性学・
トキシコゲノミクス

【致死的な，あるいは死に至る毒性】
　・癌になる
　・中毒死など
【死には至らないが健康な生活に障害となる毒性】
　・記憶が悪くなる
　・目が見えなくなる
　・耳が聞こえなくなる
　・早く老化する
　・貧血になる
　・感染し易くなる
　・皮膚がタダレる
　・疲れ易くなる
　・心臓が悪くなる
　・肝臓や腎臓が悪くなるなど
【子孫に影響を与える毒性】
　・子どもができなくなる
　・子どもの行動が異常になる
　・先天的な障害のある子が産まれるなど

図1. 毒性学の対象

毒性学は，身の回りの物質が引き起こす障害を予測し，その発生を未然に防ぐことを目的としている．トキシコゲノミクス（毒性ゲノミクス）は，最先端の網羅的遺伝子発現解析技術を用いて，従来の毒性学の予測の精度を著しく向上，迅速化させることで，国民の健康安全の確保にさらに貢献することを目指している．

中である．カクテルとも共同研究ベースで供給可能である（連絡先：kanno@nihs.go.jp）．また，ERCC（The External RNA Control Consortium）と連絡をとるとともに，国際的標準化への関与を深めるため平成18年度厚労科研費「医薬品などの有効性・安全性評価に資する遺伝子発現解析の国際的標準化に関わる研究（H18-特別-指定-023）」を立ち上げた．現在，この他にシックハウス症候群を考慮した低用量域での吸入毒性トキシコゲノミクス，1匹のマウスから多臓器を採取しそれらの連携状況をトランスクリプトームから解析する多臓器トキシコゲノミクスを開始し，特徴的な遺伝子について組織内の発現分布を *in situ* ハイブリダイゼーションで確認する作業を並行している．また，下記の3次元データをweb公開するサーバを整備し，一部の化合物から3次元多層（Millefeuille）データを順次閲覧可能とした（http://toxicomics. nihs.go.jp/db/）．

II. 3次元多層（Millefeuille）データシステム：生物系研究者に優しいデータ可視化と解析

医薬品を含む毒性既知の90化合物について単回経口投与後のトランスクリプトームデータを取得して，初期応答遺伝子カスケードを解析するための基盤データベースを構築した．現在，第二段階として反復暴露データ集積を開始し

た．データは，用量軸，時間軸，および遺伝子発現軸から成る3次元表示により，遺伝子発現の用量および時間に依存した変化を1枚の曲面として表すことで可視的に変化を判別しやすいように配慮した（図2）．これにより，コンピュータが選び出した遺伝子クラスターの中身を確認する際，特に，mRNAの合成分解のスピードなどの知見から生物学的にありえないパターン（用量軸の方向にも時間軸の方向にもジグザグな変化など）を排除する際に威力を発揮している．

1つの実験から排出されるGeneChip約50枚のデータを一括処理する能力を持ったPercellome自動換算・データ品質管理（QC）に関わるソフトウエアに加えて，3次元多層（Millefeuille）データに最適化した，発現パターン類似性による候補遺伝子検索，およびそれを発展させた教師無しクラスタリング[3]を中心とした解析システム（MF System, MFシリーズ，開発：相﨑健一）を独自に実用化し，開発継続中である（図3）．これらにより，データQCはその日のうちに，基本的な発現情報検索から全遺伝子の教師無しクラスタリングまでを3日間で完遂できるものとなっている．

この基本解析を用いて，発現パターンによって分類された候補遺伝子リストが多数生成される．一部の幸運な例ではただちに新規と思われる毒性関連反応を見いだすことができた．またそうでない場合のための1つの補強手段とし
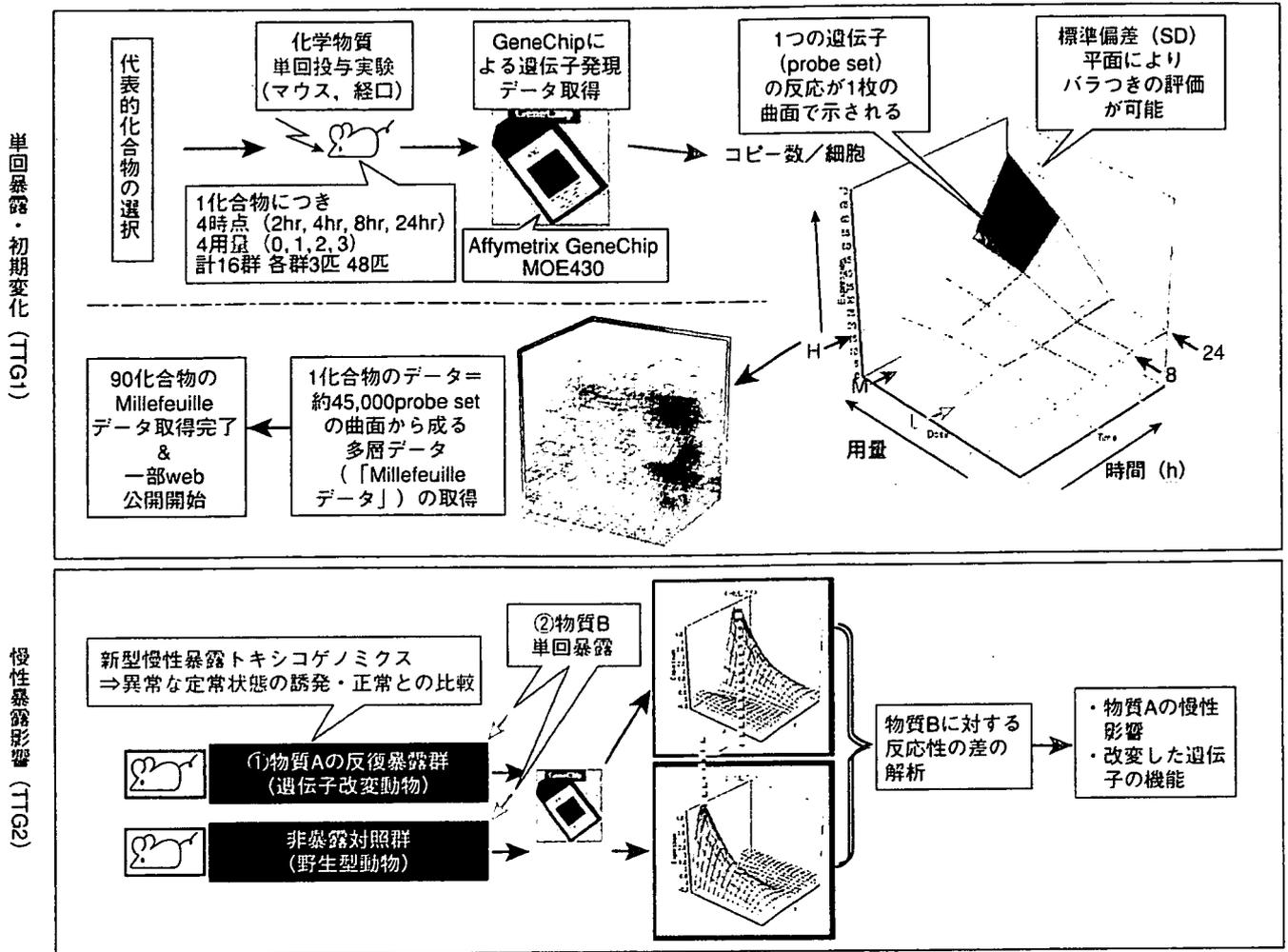
図2. Percellome法と3次元表示による多層（Millefeuille）データシステムを用いたプロジェクトの根幹部分の概要
単回投与による遺伝子発現初期変化データを90化合物について取得（上段）. 現在, 反復投与の影響を検討中（下段）. H；高用量 (high), M；中用量 (medium), L；低用量 (low), C；コントロール (control).
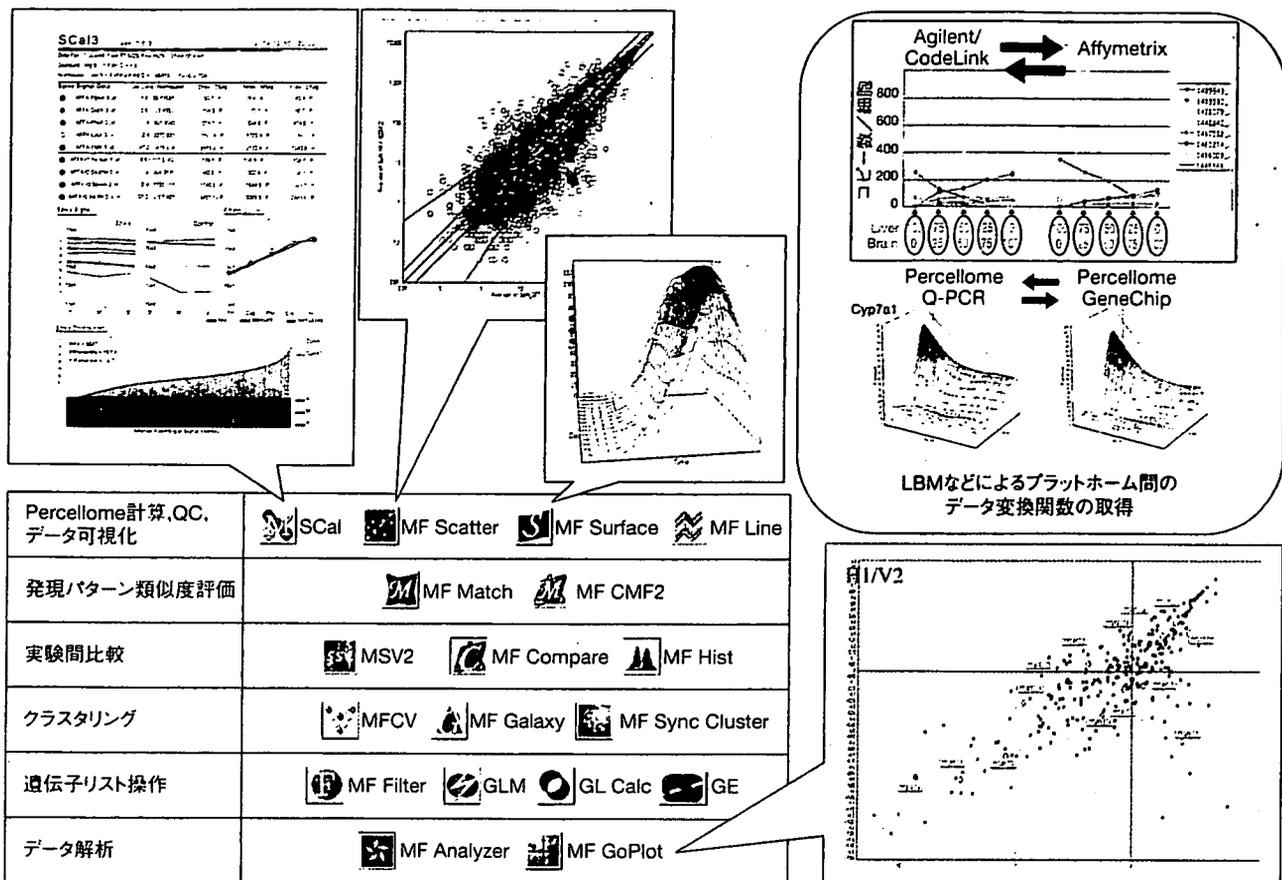
て, Gene Ontologyなどの既存知識を利用して候補遺伝子リストの理解を支援するソフトウエア（MF GoPlot）を用意した. このツールは一種の化合物クラスタリングとしても利用することができる.

さらに候補遺伝子リストを基に複数化合物間比較を行い, 複数条件下においても同期して発現する遺伝子群を自動抽出するシステムも開発済みである. 本システムで得られた同期遺伝子群はシグナルカスケードの構成単位である可能性があり, データベース化しつつ, その解析を進めている（5TB規模のデータベース部分および, 大量計算アルゴリズム実装は（株）NTTコムウェアおよび（株）日本NCR/Teradataとの共同開発による）.

Ⅲ. Percellome手法のリアルタイムPCRを含む他のプラットホームへの適用

Percellome手法は, GSCの受け入れ条件を整えることに

より, 様々なプラットホームに適用可能である. その1つとして最も定量性が高いとされるリアルタイムPCR（ABI PRISM 7900 HT・96ウェルプレート）への適用例を示す. 現行のRT-PCR絶対定量法では, 遺伝子ごとに検量線が必要であり, 多数のサンプルについて多数の遺伝子を検討するには不向きである. Percellome RT-PCRでは, マイクロアレイと同様の原理を用いる. すなわち, サンプル破砕液に, その細胞数に比例する量のスパイクカクテル(GSC)を添加し, それらのCt値をPCRプレートごとの検量線とすることにより, 測定したい遺伝子のCt値を細胞1個当たりのmRNAコピー数に換算する. これにより, GAPDHやActinなどのハウスキーピング遺伝子が変動してしまう際の問題, 例えば, 少数の遺伝子を検討する際にGlobal normalization法を適用し難い問題などが解決される. 共通サンプルを測定しデータを比較することにより, Affymetrix GeneChipのPercellome結果と9割程度の整合性が確認され,

図3. 3次元多層（Millefeuille）データの解析などに用いる独自開発プログラム群

品質管理とともにPrecellome計算を自動的に実施するSCal, Plotソフトウエア, 3次元曲面の描画ソフト（MF Surface）, など. 右上はプラットホーム間のデータ変換情報の得方を示す. LBMを用いる方法（上段）と, 実際の実験サンプルを用いる方法（下段）がある. いずれも, 一度, 両方のプラットホームでそれらのサンプルを測定する必要がある.

GeneChipとPercellome RT-PCRとの間でのコピー数の換算式がいくつかの遺伝子について得られている. この他に, Agilent社製の単色マイクロアレイとCodeLinkアレイにGSCを測定可能なカスタムアレイを用意し終え, LBMサンプルのデータなどをもとに, これらとの間の換算式も得つつある（図3右上）.

Percellome法は, Affymetrixの新しいエキソンアレイの定量性・直線性の検討にも適応可能である. Affymetrix社のHuman Exon 1.0 ST Arrayと従来型の発現アレイHuman Genome U133 plus 2について, 性質の異なるヒト癌細胞株2株から調製したLBM様標準サンプル（100：0, 75：25, 50：50, 25：75および0：100混合5サンプル）による比較を行い, 両アレイ間の相関性の高いprobe setを多数検出することができた. また, 既知のエキソンに対して設計されたprobe setでは発現が見られ, イントロンに対して設計されたprobe setでは発現が見られない, あるいは, 既知のsplicing variantに対応したprobe setの発現が検出された,

などの基本性能が確認された. しかし, Percellome法を適用して未知のsplicing variantの検出力を向上させるためには, 現状では各エキソン間の定量性に問題があることが示唆された. 定量値を算出する補正アルゴリズムの開発など, 何らかの対策が必要であることが考えられ, 現在, Affymetrix社に確認を行っている.

IV. 核内受容体原性毒性のPercellomeトキシコゲノミクス解析

受容体原性毒性とは, 化学物質が受容体（リガンド依存的転写因子を含む）に選択的に結合してシグナルをかく乱し, その結果生じる有害性を指す. 代表例としてはダイオキシンが挙げられる. AhR（Arylhydrocarbon receptor）ノックアウトマウスでは, ダイオキシンを大量に投与しても毒性がほとんど観察されない. すなわち, 野生型マウスがダイオキシンで死ぬメカニズムには, AhRが必須であり, AhRからの異常なシグナルがマウスを死に至らせていることに
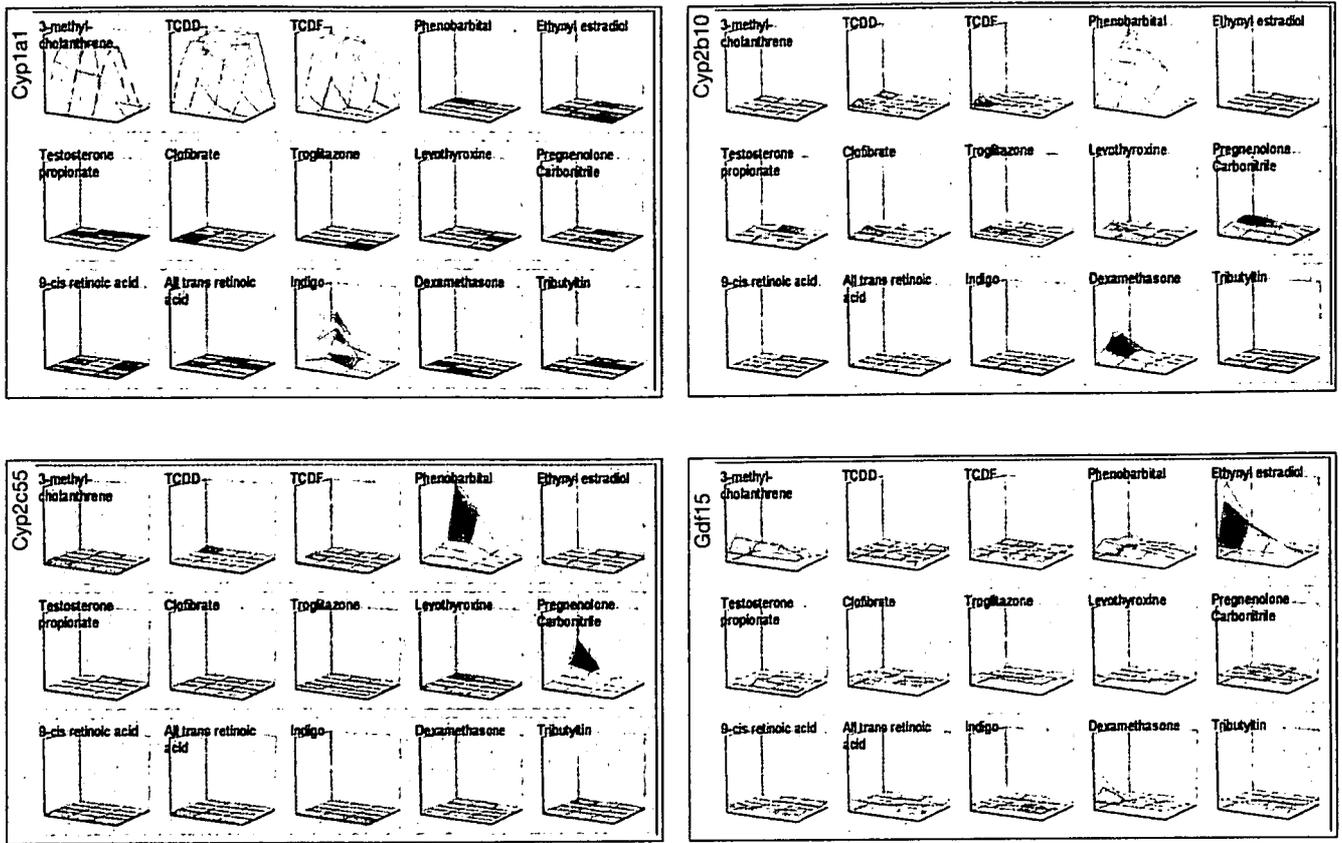
図4. 化合物間の発現比較

15種類の核内受容体リガンド化合物（各3次元グラフ内に表示）によるCyp1a1（左上）、Cyp2c55（左下）、Cyp2b10（右上）および、Gdf15（右下）の遺伝子発現を3次元表示したもの. 各軸は、図2のとおり. 縦軸のスケールは遺伝子ごとに共通. リガンドに選択的な遺伝子の発現が確認される.
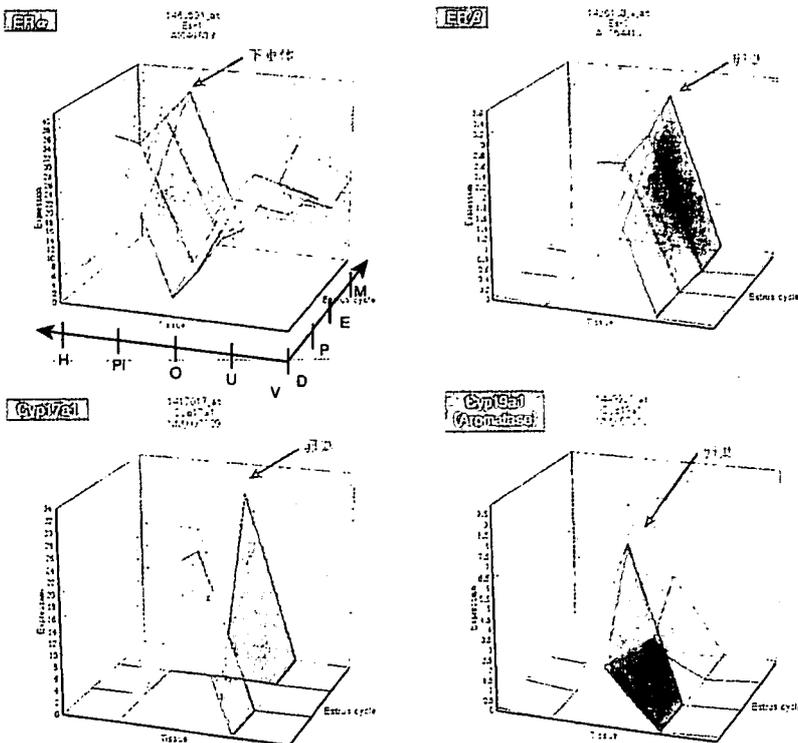

図5. 臓器間の発現比較

マウスの性周期（Diestrus, Proestrus, Estrus, Metestrusの4日間で1周期）ごとの視床下部（H）、下垂体（Pi）、卵巣（O）、子宮（U）および腟（V）における、ERα、ERβ、Cyp17a1（steroid-17α-hydroxylase）、およびCyp19a1（Aromatase）の遺伝子発現変動を3次元表示したもの. 後二者の酵素は卵巣において周期性を持って発現している.